Traveling Waves in a One-Dimensional Elastic Continuum Model of Cell Layer Migration with Stretch-Dependent Proliferation: Supplementary Material

Tracy L. Stepien[†] and David Swigon[‡]

In this Supplementary Material, we provide appendices to our paper. In Appendix A we present the adaptive finite difference method used to numerically solve the material formulation; in Appendix B we provide additional numerical simulations of the material formulation; in Appendix C we describe the procedure for conversion between the material and spatial formulations; and in Appendix D we provide additional traveling wave stability figures.

Appendix A. Numerical Method for Material Formulation. An adaptive finite difference method can be used to numerically solve the material formulation from Section 3,

$$\frac{\partial x(s,t)}{\partial t} = \frac{1}{b}\left(\frac{\partial x(s,t)}{\partial s}\right)^{-1}\frac{\partial}{\partial s}\phi\left(\frac{1}{g(s,t)}\frac{\partial x(s,t)}{\partial s}-1\right), \qquad 0\le s\le 1,\ 0\le t, \tag{A.1a}$$

$$\frac{\partial g(s,t)}{\partial t} = \gamma\left(\frac{\partial x(s,t)}{\partial s}g(s,t)^{-1}-1\right)g(s,t), \qquad 0\le s\le 1,\ 0\le t, \tag{A.1b}$$

$$x(s,0) = s, \qquad 0\le s\le 1, \tag{A.1c}$$

$$g(s,0) = 1, \qquad 0\le s\le 1, \tag{A.1d}$$

$$x(0,t) = 0, \qquad 0\le t, \tag{A.1e}$$

$$\phi\left(\epsilon(1,t)\right) = F, \qquad 0< t, \tag{A.1f}$$

for a given cell proliferation function γ, elasticity function $f=\phi(\epsilon)$, and parameters k, b, and F. It is based on the finite difference method of Mi et al. [2].

Let $\Delta t>0$ be a given step size and $t_i=(i-1)\Delta t,\ \ i=1,2,3,\ldots$. Let

$$0=s_1<s_2<\cdots<s_j<s_{j+1}<\cdots<s_{N_1}=1$$

be the initial uniform or nonuniform mesh of $[0,1]$, where N_i denotes the number of space steps in the mesh at a given time step t_i. Let x_i^j denote the numerical approximation of the cell position $x(s_j,t_i)$, and let g_i^j denote the numerical approximation of the growth gradient $g(s_j,t_i)$.

A nonadaptive finite difference method results in erroneous exponential growth at the cell layer moving edge due to the moving boundary and expanding mesh. Let TOL denote a maximum allowed distance between any two cells. At time step t_i, if any two cells at positions x_i^j and x_i^{j+1} for some j are further apart than TOL, we add a new mesh point halfway between

[†]Department of Mathematics, University of Pittsburgh, Pittsburgh, PA 15260.
Present address: School of Mathematical and Statistical Sciences, Arizona State University, Tempe, AZ 85287 (tstepien@asu.edu). This author's work was supported by NSF award EMSW21-RTG 0739261 and an Andrew Mellon Predoctoral Fellowship.
[‡]Department of Mathematics, University of Pittsburgh, Pittsburgh, PA 15260 (swigon@pitt.edu).

s_j and s_{j+1} and linearly interpolate the position x and growth gradient g at the new mesh point. The new mesh is used for time step t_{i+1}.

Various elasticity functions $f = \phi(\epsilon)$ can be assumed, but for a concrete example assume $f = \phi(\epsilon) = k\ln(\epsilon + 1)$, and define parameters $\kappa = k/b$ and $\varphi = F/k$. Recall from equation (2.2) in Section 2 that $\epsilon = \frac{\partial x}{\partial s}\frac{1}{g} - 1$.

The initial conditions imply, for $1 \le j \le N_i$,

$$x_1^j = s_j, \qquad g_1^j = 1, \qquad \epsilon_1^j = 0. \tag{A.2}$$

Equation (A.1b) is solved first using explicit difference with a mixed discretization for the right hand side, for $1 \le j \le N_i$,

$$g_{i+1}^j = \frac{g_i^j}{1 - \Delta t\rho(\epsilon_i^j)}. \tag{A.3}$$

Centered difference is used for ϵ in the interior and explicit difference for the boundaries, and because the right boundary is constant, for $i \ge 2$ and $2 \le j \le N_i - 1$,

$$\epsilon_i^j = \left(\frac{x_i^{j+1} + (\alpha^2 - 1)x_i^j - \alpha^2 x_i^{j-1}}{(\alpha+1)(s_{j+1} - s_j)}\right)\frac{1}{g_i^j} - 1, \qquad \alpha = \frac{s_{j+1} - s_j}{s_j - s_{j-1}}, \tag{A.4a}$$

$$\epsilon_i^1 = \left(\frac{x_i^2 - x_i^1}{s_2 - s_1}\right)\frac{1}{g_i^1} - 1, \tag{A.4b}$$

$$\epsilon_i^{N_i} = e^{\varphi} - 1. \tag{A.4c}$$

Equation (A.1a) is solved next, and assuming $f = \phi(\epsilon) = k\ln(\epsilon + 1)$, (A.1a) becomes

$$\frac{\partial x}{\partial t} = \kappa\left(\frac{\frac{\partial^2 x}{\partial s^2}}{\left(\frac{\partial x}{\partial s}\right)^2} - \frac{\frac{\partial g}{\partial s}}{g\frac{\partial x}{\partial s}}\right). \tag{A.5}$$

Using implicit difference in the numerator and explicit difference in the denominator to discretize the governing equation, we obtain a method that is first-order accurate in time and second-order accurate in space. For $i \ge 2$ and $2 \le j \le N_i - 1$,

$$x_{i+1}^j - x_i^j = \kappa\Delta t\left(\frac{\frac{2(s_{j+1}-s_{j-1})x_{i+1}^{j+1}}{s_{j+1}-s_j} - \frac{2(s_{j+1}-s_{j-1})^2 x_{i+1}^j}{(s_{j+1}-s_j)(s_j-s_{j-1})} + \frac{2(s_{j+1}-s_{j-1})x_{i+1}^{j-1}}{s_j - s_{j-1}}}{(x_i^{j+1} - x_i^{j-1})^2} - \frac{g_{i+1}^{j+1} - g_{i+1}^{j-1}}{g_i^j(x_i^{j+1} - x_i^{j-1})}\right), \tag{A.6}$$

which, after rearranging, becomes

$$\eta_j M_i^j x_{i+1}^{j+1} - (\sigma_j M_i^j + 1)x_{i+1}^j + \mu_j M_i^j x_{i+1}^{j-1} = -x_i^j + u_i^j, \tag{A.7}$$

where we define

$$M_i^j = \kappa \Delta t \left(\frac{2}{(x_i^{j+1} - x_i^{j-1})^2} \right), \tag{A.8a}$$

$$u_i^j = \kappa \Delta t \left(\frac{g_{i+1}^{j+1} - g_{i+1}^{j-1}}{g_i^j (x_i^{j+1} - x_i^{j-1})} \right), \tag{A.8b}$$

$$\eta_j = \frac{s_{j+1} - s_{j-1}}{s_{j+1} - s_j}, \tag{A.8c}$$

$$\sigma_j = \frac{(s_{j+1} - s_{j-1})^2}{(s_{j+1} - s_j)(s_j - s_{j-1})}, \tag{A.8d}$$

$$\mu_j = \frac{s_{j+1} - s_{j-1}}{s_j - s_{j-1}}. \tag{A.8e}$$

The boundary conditions imply, for $i \geq 2$,

$$x_i^1 = 0, \tag{A.9a}$$

$$x_i^{N_i} = x_i^{N_i - 1} + (s_{N_i} - s_{N_i - 1}) g_i^{N_i} e^{\varphi}, \tag{A.9b}$$

and the solution x_{i+1}^j at the time step t_{i+1} can be found by solving the linear system

$$A \begin{pmatrix} x_{i+1}^2 \\ x_{i+1}^3 \\ \vdots \\ x_{i+1}^{N_i - 2} \\ x_{i+1}^{N_i - 1} \end{pmatrix} = \begin{pmatrix} -x_i^2 + u_i^2 \\ -x_i^3 + u_i^3 \\ \vdots \\ -x_i^{N_i - 2} + u_i^{N_i - 2} \\ -x_i^{N_i - 1} + u_i^{N_i - 1} - \eta_{N_i - 1}(s_{N_i} - s_{N_i - 1}) M_i^{N_i - 1} g_{i+1}^{N_i} e^{\varphi} \end{pmatrix}, \tag{A.10}$$

where A is the tridiagonal matrix

$$\begin{pmatrix} -(\sigma_2 M_i^2 + 1) & \eta_2 M_i^2 & 0 & \cdots & 0 \\ \mu_3 M_i^3 & -(\sigma_3 M_i^3 + 1) & \eta_3 M_i^3 & \cdots & 0 \\ \vdots & \ddots & \ddots & \ddots & \vdots \\ 0 & \cdots & \mu_{N_i - 2} M_i^{N_i - 2} & -(\sigma_{N_i - 2} M_i^{N_i - 2} + 1) & \eta_{N_i - 2} M_i^{N_i - 2} \\ 0 & \cdots & 0 & \mu_{N_i - 1} M_i^{N_i - 1} & -(\sigma_{N_i - 1} M_i^{N_i - 1} + 1) + \eta_{N_i - 1} M_i^{N_i - 1} \end{pmatrix}. \tag{A.11}$$

This numerical method is first-order accurate in time and second-order accurate in space (Stepien [3]). The stability of the method without adaptive mesh refinement can be analyzed to approximate the behavior of the nonlinear method using techniques for linear methods. Without cell proliferation (i.e. $\gamma = 0$), the method is expected to be unconditionally stable, but with nonzero cell proliferation, the method is expected to be conditionally stable.

Appendix B. Additional Numerical Simulations. Figure B.1 shows the evolution of the cell layer for zero cell proliferation function $\gamma(\epsilon) = 0$ and linear cell proliferation function $\gamma(\epsilon) = \epsilon$ with the linear elasticity function $f = \phi(\epsilon) = k\epsilon$ and reciprocal elasticity function $f = \phi(\epsilon) = k\left(1 - \frac{1}{\epsilon+1}\right)$.

Appendix C. Equivalence Between the Material and Spatial Formulations. There is an equivalence between material and spatial coordinates through point-particle interchangeability. In the material coordinate description, $x = x(s,t)$, and in the spatial coordinates description, $s = s(x,t)$, and therefore we have $x(s(x,t),t) = x$ and $s(x(s,t),t) = s$. We will also use the notation $\tilde{\rho}(s,t) = \rho(x(s,t),t)$, where $\tilde{\rho}$ is the density of cells in material coordinates defined as

$$\tilde{\rho}(s,t) = \rho_0 \left(\frac{\partial x(s,t)}{\partial \hat{s}}\right)^{-1}. \tag{C.1}$$

Note that (C.1) and $\epsilon = \frac{\partial x}{\partial \hat{s}} - 1$ imply

$$\epsilon(s,t) = \frac{\rho_0}{\tilde{\rho}(s,t)} - 1. \tag{C.2}$$

Governing Equations and Elasticity Functions. The equation relating the velocity of the cells and the gradient of the cell density,

$$\frac{\partial x}{\partial t} = -\frac{1}{b} p'(\rho) \frac{\partial \rho}{\partial x}, \tag{C.3}$$

holds for the spatial formulation. Evaluating (C.3) at $x = x(s,t)$,

$$\frac{\partial x}{\partial t} = -\frac{1}{b} p'(\tilde{\rho}) \frac{\partial \tilde{\rho}}{\partial x} = -\frac{1}{b} \frac{\partial}{\partial x}(p(\tilde{\rho})) = -\frac{1}{b} \frac{\partial s}{\partial x} \frac{\partial}{\partial s}(p(\tilde{\rho})) = -\frac{1}{b} \frac{\partial p(\tilde{\rho})/\partial s}{\partial x/\partial s}, \tag{C.4}$$

which is the same equation as (A.1a) since

$$f(s,t) = -p(\tilde{\rho}(s,t)). \tag{C.5}$$

From this we obtain the conversion formulas in Section 5,

$$\phi(\epsilon) = -p\left(\frac{\rho_0}{\epsilon+1}\right), \qquad p(\rho) = -\phi\left(\frac{\rho_0}{\rho} - 1\right), \tag{C.6}$$

implying that we have equivalence between the governing equations of the two formulations.

The equivalent spatial coordinates logarithmic, linear, and reciprocal cell layer elasticity functions from Section 2 are, respectively,

$$p(\rho) = k \ln\left(\frac{\rho}{\rho_0}\right), \tag{C.7a}$$

$$p(\rho) = k\left(1 - \frac{\rho_0}{\rho}\right), \tag{C.7b}$$

$$p(\rho) = k\left(\frac{\rho}{\rho_0} - 1\right). \tag{C.7c}$$

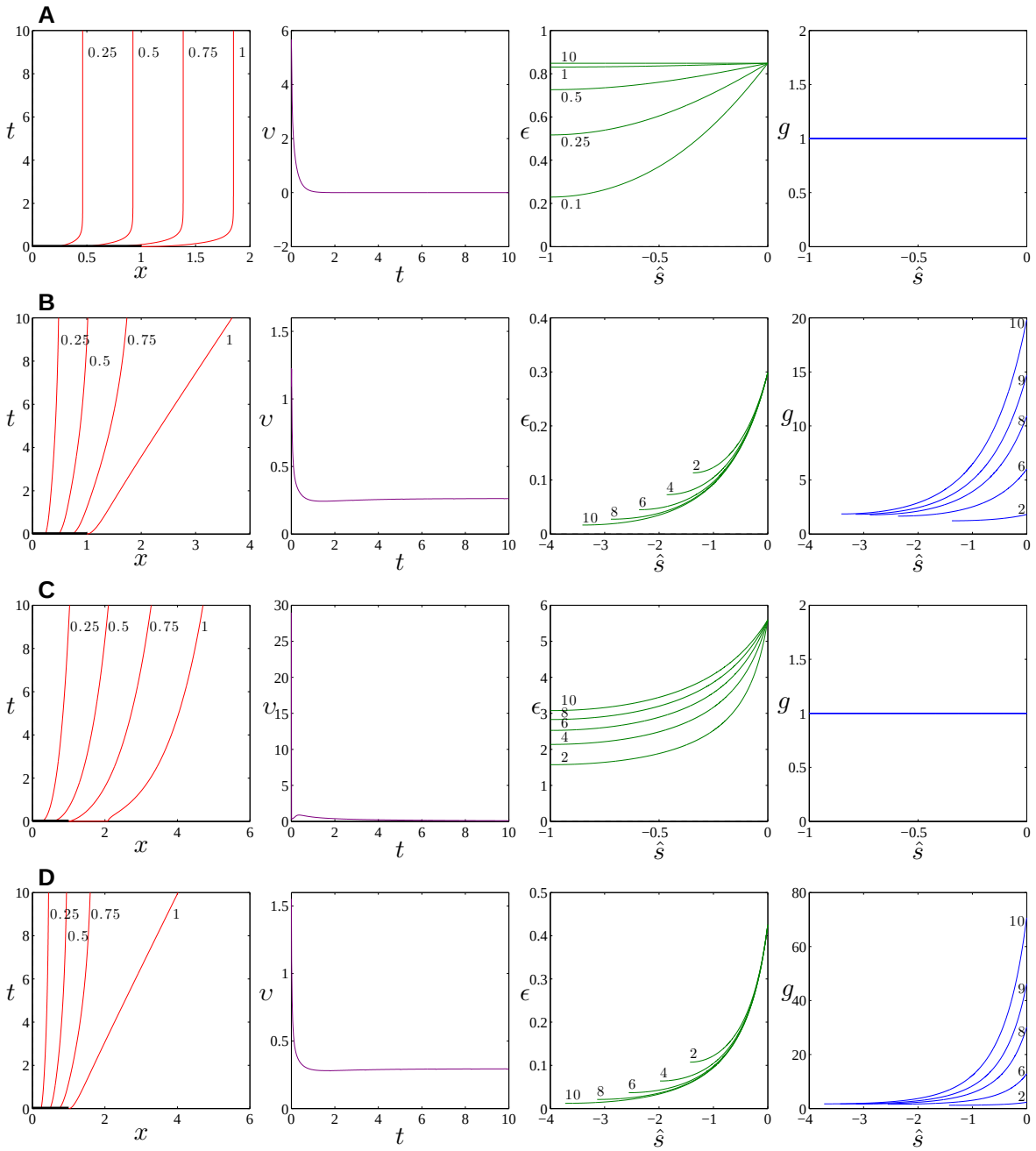

Figure B.1. *Numerical solution of the model equations with (A)–(B) the linear elasticity function and (C)–(D) the reciprocal elasticity function. See Figure 3 in the main text for a description of each column. (A),(C) No growth* $\gamma(\epsilon) = 0$, $k = 2.947$, $b = 1$, $F = 2.5$*; and (B),(D) linear growth function,* $k = 0.838$, $b = 1$, $F = 0.25$.

Cell Proliferation Functions. To derive the relation between γ and q, we note that the law of conservation of cell number (mass) in spatial coordinates is

$$\frac{\partial \rho(x,t)}{\partial t} = -\frac{\partial}{\partial x}\left(\rho(x,t)\frac{\partial x}{\partial t}\right) + q(\rho(x,t)), \tag{C.8}$$

and the material derivative is

$$\frac{\partial \rho(x(s,t),t)}{\partial t} = \frac{\partial \rho(x,t)}{\partial x}\bigg|_{x=x(s,t)} \frac{\partial x(s,t)}{\partial t} + \frac{\partial \rho(x,t)}{\partial t}\bigg|_{x=x(s,t)}, \tag{C.9}$$

which is equivalent by notation to

$$\frac{\partial \tilde{\rho}(s,t)}{\partial t} = \rho_0 \left(\frac{\partial x(s,t)}{\partial s}\right)^{-1} \frac{\partial^2 \hat{s}(s,t)}{\partial s \partial t} - \rho_0 \frac{\partial \hat{s}(s,t)}{\partial s}\left(\frac{\partial x(s,t)}{\partial s}\right)^{-2} \frac{\partial^2 x(s,t)}{\partial s \partial t}. \tag{C.10}$$

Equating the right hand sides of the last two equations (C.9) and (C.10),

$$\begin{aligned}\frac{\partial \rho(x,t)}{\partial t}\bigg|_{x=x(s,t)} = \rho_0 \left(\frac{\partial x(s,t)}{\partial s}\right)^{-1} \frac{\partial^2 \hat{s}(s,t)}{\partial s \partial t} - \rho_0 \frac{\partial \hat{s}(s,t)}{\partial s}\left(\frac{\partial x(s,t)}{\partial s}\right)^{-2} \frac{\partial^2 x(s,t)}{\partial s \partial t} \\ - \frac{\partial \rho(x,t)}{\partial x}\bigg|_{x=x(s,t)} \frac{\partial x(s,t)}{\partial t},\end{aligned} \tag{C.11}$$

which is the left hand side of (C.8) evaluated at $x = x(s,t)$. The right hand side of (C.8) evaluated at $x = x(s,t)$ is

$$\begin{aligned}&-\rho(x,t)|_{x=x(s,t)} \left(\frac{\partial x(s,t)}{\partial s}\right)^{-1} \frac{\partial}{\partial s}\left(\frac{\partial x(s,t)}{\partial t}\right) - \frac{\partial x(s,t)}{\partial t}\frac{\partial \rho(x,t)}{\partial x}\bigg|_{x=x(s,t)} + q(\rho(x,t))|_{x=x(s,t)} \\ &= -\rho_0 \left(\frac{\partial x(s,t)}{\partial s}\right)^{-2} \frac{\partial \hat{s}(s,t)}{\partial s}\frac{\partial^2 x(s,t)}{\partial s \partial t} - \frac{\partial x(s,t)}{\partial t}\frac{\partial \rho(x,t)}{\partial x}\bigg|_{x=x(s,t)} + q(\rho(x,t))|_{x=x(s,t)}.\end{aligned} \tag{C.12}$$

Thus, equating (C.11) and (C.12) and evaluating at $x = x(s(x,t),t)$, we conclude that

$$q(\tilde{\rho}(s,t)) = \rho_0 \left(\frac{\partial x(s,t)}{\partial s}\right)^{-1} \frac{\partial^2 \hat{s}(s,t)}{\partial s \partial t}. \tag{C.13}$$

Since $g(s,t) = \frac{\partial \hat{s}(s,t)}{\partial s}$ by definition, then $\frac{\partial g(s,t)}{\partial t} = \frac{\partial^2 \hat{s}(s,t)}{\partial s \partial t}$, and in view of (A.1b),

$$\frac{\partial^2 \hat{s}(s,t)}{\partial s \partial t} = \gamma(\epsilon(s,t))g(s,t). \tag{C.14}$$

Therefore, substituting (C.14) into (C.13) and recalling (C.2), we obtain the conversion formulas in Section 5,

$$\gamma(\epsilon) = \frac{\epsilon+1}{\rho_0} q\left(\frac{\rho_0}{\epsilon+1}\right), \qquad q(\rho) = \rho\gamma\left(\frac{\rho_0}{\rho} - 1\right). \tag{C.15}$$

The spatial coordinates equivalents to the material coordinates linear, Fisher, and cubic growth functions from Section 2 are, respectively,

$$q(\rho) = \rho_0 - \rho, \tag{C.16a}$$

$$q(\rho) = \rho\left(1 - \frac{\rho}{\rho_0}\right), \tag{C.16b}$$

$$q(\rho) = -\frac{\rho_0}{\rho^2}(\rho_0 - \rho)\left(\rho_0 - 2\rho\right). \tag{C.16c}$$

Growth Gradient. The spatial formulation of Arciero et al. [1] does not include an expression for the growth gradient. Let us introduce the notation $g(s,t) = \widehat{g}(x(s,t),t)$, where $\widehat{g}$ is the growth gradient in spatial coordinates. Taking the partial derivative of both sides of $g(s,t) = \widehat{g}(x(s,t),t)$ with respect to t, from (A.1b) and the material derivative we obtain

$$\gamma(\epsilon(s,t))g(s,t) = \left.\frac{\partial \widehat{g}(x,t)}{\partial x}\right|_{x=x(s,t)} \frac{\partial x(s,t)}{\partial t} + \left.\frac{\partial \widehat{g}(x,t)}{\partial t}\right|_{x=x(s,t)}. \tag{C.17}$$

From (C.15), we derive

$$\gamma(\epsilon(s,t)) = \frac{1}{\tilde{\rho}(s,t)} q(\tilde{\rho}(s,t)). \tag{C.18}$$

From (A.1a) and by definitions,

$$\begin{aligned}\frac{\partial x}{\partial t} &= \frac{1}{b}\left(\frac{\partial x}{\partial s}\right)^{-1}\frac{\partial f}{\partial s} = -\frac{1}{b}\left(\frac{\partial x}{\partial \hat{s}}\frac{\partial \hat{s}}{\partial s}\right)^{-1}\frac{\partial}{\partial s}(p(\tilde{\rho})) = -\frac{1}{b}\left(\frac{\partial x}{\partial \hat{s}}\frac{\partial \hat{s}}{\partial s}\right)^{-1}\frac{dp(\tilde{\rho})}{d\tilde{\rho}}\frac{\partial \tilde{\rho}}{\partial x}\frac{\partial x}{\partial \hat{s}}\frac{\partial \hat{s}}{\partial s} \\ &= -\frac{1}{b}\frac{dp(\tilde{\rho})}{d\tilde{\rho}}\frac{\partial \tilde{\rho}}{\partial x}.\end{aligned} \tag{C.19}$$

Substituting (C.18) and (C.19) into (C.17) and evaluating at $s = s(x,t)$, we obtain the following partial differential equation for $\widehat{g}$,

$$\frac{\partial \widehat{g}}{\partial t} - \frac{1}{b}p'(\rho)\frac{\partial \widehat{g}}{\partial x} - \frac{q(\rho)}{\rho}\widehat{g} = 0. \tag{C.20}$$

Initial and Boundary Conditions. Lastly, to derive the equivalent initial and boundary conditions for the spatial formulation compared to the material formulation (A.1c)–(A.1f), define $X(t)$ as the position of the moving edge in spatial coordinates. Assuming the cell layer is initially uniform and free from internal stresses, initial condition (A.1c) via (C.1) is equivalent to $\rho(x,0) = \rho_0,\ 0 \le x \le X(0)$. Assuming the left boundary of the cell layer is fixed, boundary condition (A.1e) is equivalent to a no flux Neumann condition $\frac{\partial \rho(0,t)}{\partial x} = 0,\ 0 \le t$. Assuming the force applied at the right boundary is equal to F, boundary condition (A.1f) via (C.5) is equivalent to $p(\rho(X(t),t)) = -F,\ 0 < t$. Lastly, the speed of the moving edge $X(t)$ satisfies (C.3), so we have the boundary condition $X'(t) = -\frac{1}{b}p'(\rho(X(t),t))\frac{\partial \rho(X(t),t)}{\partial x},\ 0 < t$.

Appendix D. Additional Stability Figures. Figure D.1 shows the traveling wave stability results for the growth function $q(\rho) = (\rho_0 - \rho)(\rho_0 - 2\rho)(\rho_0 - 4\rho)$, and Figures D.2–D.3 show the

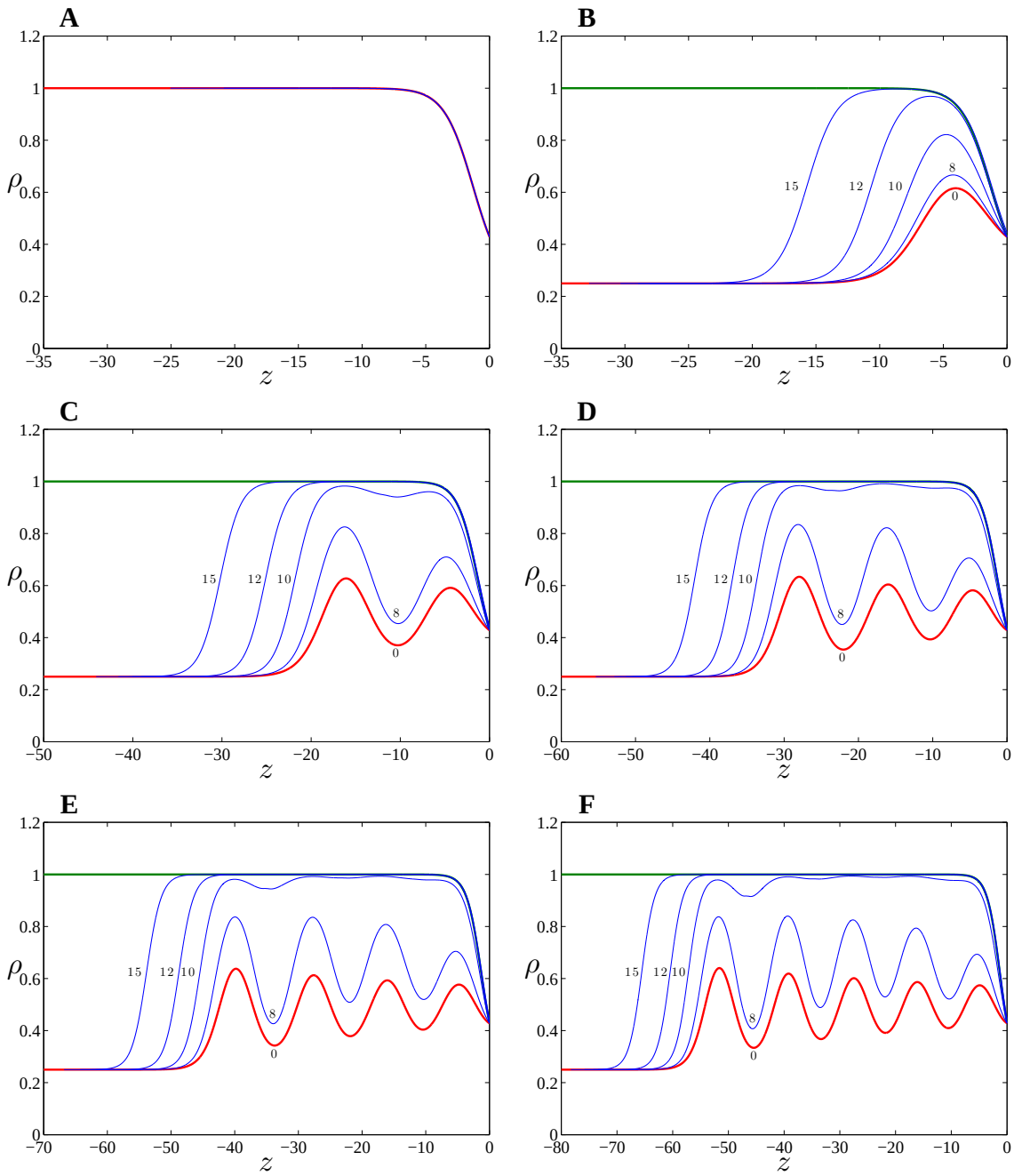

Figure D.1. *Stability of traveling waves: spatial formulation to material formulation. Growth function* $q(\rho) = (1-\rho)(1-2\rho)(1-4\rho)$ *with logarithmic elasticity function,* $k = 2.947$, $b = 1$, *and* $F = 2.5$. *The initial cell positions (red) are found using the analytic traveling wave solution corresponding to (A) 0 loops about the stable spiral with* $\rho_0 = 1$; *(B) 0 loops about the stable spiral with* $\rho_0 = \frac{1}{4}$; *(C) 1 loop about the stable spiral with* $\rho_0 = \frac{1}{4}$; *(D) 2 loops about the stable spiral with* $\rho_0 = \frac{1}{4}$; *(E) 3 loops about the stable spiral with* $\rho_0 = \frac{1}{4}$; *and (F) 4 loops about the stable spiral with* $\rho_0 = \frac{1}{4}$. *The density profiles at* $t = 8$, 10, 12, 15 *hours (blue) found numerically in the material formulation converge to the analytic traveling wave solution (green) corresponding to 0 loops about the stable spiral with* $\rho_0 = 1$.

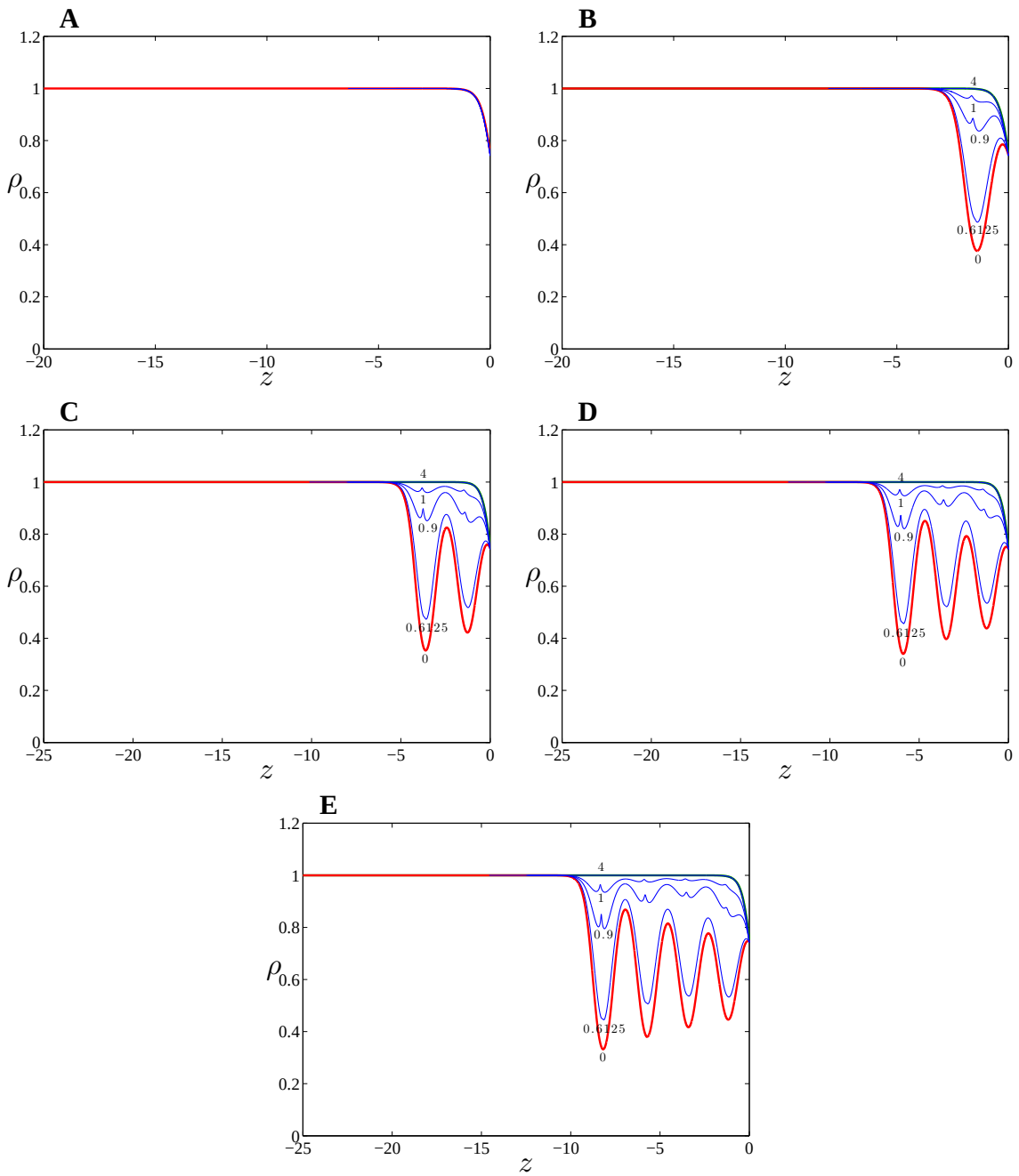

Figure D.2. *Stability of traveling waves: spatial formulation to material formulation. Growth function* $q(\rho) = (1-\rho)(1-8\rho)(3-5\rho)$ *with logarithmic elasticity function,* $k = 2.947$, $b = 1$, $F = 2.5$, *and* $\rho_0 = 1$. *The initial cell positions (red) are found using the analytic traveling wave solution corresponding to* $\rho_0 = 1$ *with the following number of loops about the stable spiral: (A) 0; (B) 1; (C) 2; (D) 3; and (E) 4. The density profiles at* $t = 0.6125,\ 0.9,\ 1,\ 4$ *hours (blue) found numerically in the material formulation converge to the analytic traveling wave solution (green) corresponding to 0 loops about the stable spiral with* $\rho_0 = 1$.

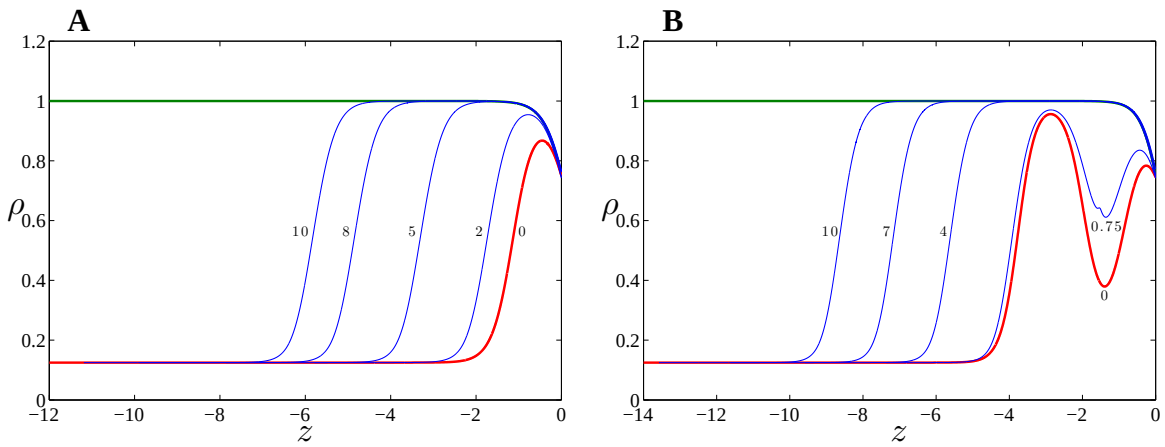

Figure D.3. *Stability of traveling waves: spatial formulation to material formulation. Growth function* $q(\rho) = (1-\rho)(1-8\rho)(3-5\rho)$ *with logarithmic elasticity function,* $k = 2.947$*,* $b = 1$*,* $F = 2.5$*, and* $\rho_0 = \frac{1}{5}$*. The initial cell positions (red) are found using the analytic traveling wave solution corresponding to* $\rho_0 = \frac{1}{8}$ *with the following number of loops about the stable spiral: (A) 0; and (B) 1. The density profiles at (A)* $t = 2, 5, 8, 10$ *hours, (B)* $t = 0.75, 4, 7, 10$ *hours (blue) found numerically in the material formulation converge to the analytic traveling wave solution (green) corresponding to 0 loops about the stable spiral with* $\rho_0 = 1$*.*

results for the growth function $q(\rho) = (\rho_0 - \rho)(\rho_0 - 8\rho)(3\rho_0 - 5\rho)$, with logarithmic elasticity function $f = \phi(\epsilon) = k\ln(\epsilon+1)$, when we use the analytic traveling wave solution of the spatial formulation as an initial condition for the material formulation numerical simulations.

Similarly to the cubic growth function, in the cases where there are two saddles, we observe different behaviors based on how many loops the solution trajectory in phase space traverses about the stable spiral. All of the solutions converge to the traveling wave solution for the trajectory that never crosses the ρ-axis. For the traveling wave solutions for the saddle on the left (Figures D.1B–F and D.3), we see that there is a "wave within a wave" such that once the solutions converge near the moving boundary ($z = 0$) to the trajectory that never crosses the ρ-axis, there is a traveling wave of density that moves to the left.

REFERENCES

[1] J. C. Arciero, Q. Mi, M. F. Branca, D. J. Hackam, and D. Swigon, *Continuum model of collective cell migration in wound healing and colony expansion*, Biophys. J., 100 (2011), pp. 535–543.

[2] Q. Mi, D. Swigon, B. Rivière, S. Cetin, Y. Vodovotz, and D. J. Hackam, *One-dimensional elastic continuum model of enterocyte layer migration*, Biophys. J., 93 (2007), pp. 3745–3752.

[3] T. L. Stepien, *Collective Cell Migration in Single and Dual Cell Layers*, Ph.D. thesis. University of Pittsburgh, Pittsburgh, PA, 2013.